

## THEORETICAL STUDY OF Si and N ADSORPTION ON THE Si-TERMINATED SiC(001) SURFACE

L. PIZZAGALLI\*

*Lawrence Livermore National Laboratory, L-415, PO Box 808,  
Livermore, CA 94550, USA*

A. CATELLANI

*CNR-MASPEC, Via Chiavari 18/A, I-43100 Parma, Italy*

G. GALLI and F. GYGI

*Lawrence Livermore National Laboratory, PO Box 808,  
Livermore, CA 94550, USA*

A. BARATOFF

*Department of Physics and Astronomy, Basel University,  
Klingelbergstr. 82, CH-4056 Basel, Switzerland*

Received 12 September 1999

We report the results of first principles molecular dynamics simulations of the adsorption of Si and N atoms on a Si-terminated  $p(2 \times 1)$  SiC(001) surface. In particular, we discuss different structural models for the Si-rich  $(3 \times 2)$  surface, and the adsorption of  $1/8$ ,  $1/2$  and 1 monolayer nitrogen on the  $p(2 \times 1)$  surface. Our simulations show that a SiC(001)- $p(2 \times 1)$  surface covered by a nitrogen monolayer is an inert substrate which inhibits growth.

### 1. Introduction

Silicon carbide is an attractive material for high temperature micro- and optoelectronic devices<sup>1</sup> because of its wide band gap, high thermal conductivity, high hardness and chemical inertness. Having a small lattice mismatch with GaN, SiC has also emerged as a promising substrate for the growth of nitride-based devices.<sup>1,2</sup>

A thorough understanding of SiC surfaces properties is an important prerequisite for successful technological applications. The Si-terminated (001) surface of the cubic SiC has been widely studied.<sup>3</sup> Deposition of extra Si on the Si-terminated  $p(2 \times 1)$  surface leads to a saturated  $(3 \times 2)$  reconstructed surface. There is still a controversy about the structure and the coverage of this reconstruction,<sup>3</sup> and

very little is known about the growth processes of, for example, nitride materials on SiC. Experimentally, the Si-SiC(001) surface is the substrate of choice<sup>4</sup> when growing cubic GaN on  $\beta$ -SiC. GaN and SiC have a small lattice mismatch and very similar mechanical and thermal properties. However, the interface between the two materials has not yet been well characterized experimentally. Furthermore most theoretical studies of SiC and nitride interfaces have concentrated on static properties of sharp interfaces.<sup>5</sup> No attempt has been made so far to dynamically model the adsorption of either Ga or N on a SiC substrate.

Here we summarize the results of several calculations of the adsorption of Si<sup>6,7</sup> and N<sup>8</sup> atoms on the Si-terminated SiC(001) surface, as obtained by

---

\*Corresponding author. E-mail: pizza@llnl.gov

performing first-principles molecular dynamics simulations both at zero and finite temperature. Our computations were done within Density Functional Theory, using the Local Density Approximation. We used pseudopotentials<sup>9</sup> and a plane wave basis set, which allowed us to perform systematic checks on the accuracy of computed quantities. The energy cutoff was 36 Ry (42 Ry) for the study of the Si (N) deposition. In order to make contact with STM experiments, the tunneling current  $I(x, y, z; V)$  and its derivative with respect to applied voltage  $V$  have been computed for selected, optimized surface geometries. The calculations have been carried out using the Tersoff–Hamman approximation,<sup>10</sup> where  $\partial I(x, y, z; V)/\partial V \propto \sum_i |\psi_i(x, y, z)|^2 f'(\varepsilon_i + eV)$ . Here  $\psi_i(x, y, z)$  and  $\varepsilon_i$  are single particle wave functions and eigenvalues, respectively,  $V$  indicates an applied voltage and  $f'$  is the derivative of the Fermi distribution. We refer the reader to the original papers for the details of our first-principles simulations.<sup>6–8</sup>

## 2. Si Adsorption

In a previous paper<sup>11</sup> we have discussed the geometries of both the  $p(2 \times 1)$  and the  $c(4 \times 2)$  reconstructions of Si–SiC(001). In agreement with Sabisch *et al.*,<sup>12</sup> we have found that the  $p(2 \times 1)$  reconstruction is characterized by dimer rows, with dimers much longer (2.6 Å) than those of Si(001) ( $\simeq 2.3$  Å). At present, this has not been confirmed experimentally, and the only fit to LEED data available in the literature points at shorter dimers.<sup>13</sup> However, very recent ARUPS data<sup>14</sup> are consistent with models

implying a weak bonding of the Si dimers. Furthermore, we have found<sup>11</sup> that strained SiC samples exhibit a  $c(4 \times 2)$  surface geometry, characterized by alternating unbuckled short and long dimers, the short dimers having a component perpendicular to the surface smaller than the long ones. The dimer bond lengths are 2.54 and 2.62 Å in the case, for example, of a 3% strained bulk. This surface geometry is in agreement with the alternating-up-and-down-dimer (AUDD) model proposed on the basis of STM experiments.<sup>15–17</sup>

In our study of Si adsorption on SiC(001), we first considered a Si ad-atom and optimized two different surface geometries, with an extra atom between and on top of  $p(2 \times 1)$  dimer rows, respectively. The configuration of minimum energy corresponds to the adatom sitting between rows, at 0.9 Å from the surface and forming four long (2.50 Å), equivalent backbonds with the surface atoms (see Fig. 1). In Si–SiC(001) the distance between rows is much smaller than in Si(001), and thus the adatom can find a symmetric site between rows. On the contrary, an adatom on Si(001) privileges a specific row, forming only three back-bonds, two with atoms of the first surface layer and one with an atom of the second surface layer.<sup>18</sup> The presence of an adatom on Si–SiC(001) causes the surface tension to increase by a few percent.

We then considered ad-dimers on a  $p(2 \times 1)$  terminated surface in order to determine a stable geometry. Recent measurements<sup>19</sup> suggest that these ad-dimers are perpendicular to the rows, in agreement with the results of *ab initio* calculations.<sup>20</sup>

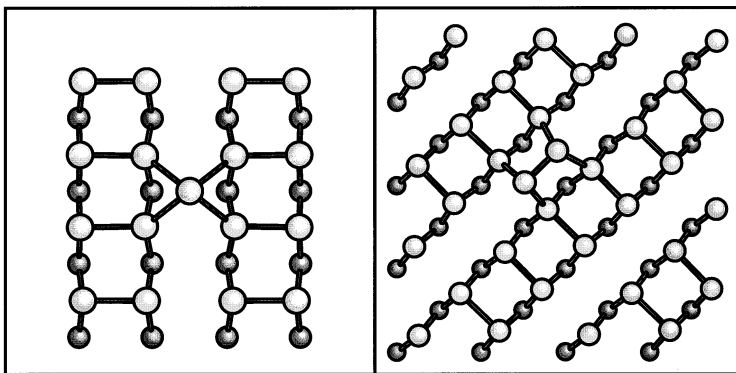


Fig. 1. Geometries of an ad-atom (left panel) and an ad-dimer (right panel) on top of a Si–SiC(001) surface, as optimized in our calculations (see text). Black and white spheres represent C and Si atoms, respectively.

On the other hand STM experiments<sup>21</sup> have reported lines of dimers on Si-SiC(001) being parallel to  $p(2 \times 1)$  dimer rows, and this could suggest an ad-dimer geometry parallel to the rows. We have considered an ad-dimer *between* rows and optimized the total energy for geometries parallel<sup>22</sup> and perpendicular to the  $p(2 \times 1)$  dimer rows. We have found that the perpendicular ad-dimer has a total energy about 0.6 eV lower than the parallel one. We note that the ad-dimer bond length is much smaller than those of surface dimers, 2.28 Å, and thus the chemical bond of the ad-dimer is expected to be rather different from that of the weak, much longer surface dimers. The two atoms of the ad-dimer, which is buckled, form respectively two bonds of about 2.35 Å and 2.38 Å with surface atoms and sit at  $\simeq 1.4$  Å and  $\simeq 1.7$  Å from the surface.

Further deposition of Si atoms on  $p(2 \times 1)$  Si-SiC(001) leads to the saturated  $(3 \times 2)$  reconstruction. Three different atomic configurations, depicted in Fig. 2, have been suggested in the literature. In the Double Dimer-Row (DDR) model, proposed by Dayan<sup>23</sup> and apparently supported by other experimental studies,<sup>24–27</sup> there are two Si ad-dimers on top of the full Si layer [Fig. 2(a)]. The resulting coverage  $\theta_{\text{Si}} = \frac{2}{3}$  is in contradiction with the measured  $\theta_{\text{Si}}$  value of  $\frac{1}{3}$  claimed by several groups.<sup>28–30</sup> The straightforward extension of this model to the  $(5 \times 2)$  reconstruction is also inconsistent with the measured coverage.<sup>29</sup> Moreover, this model is not supported by some STM studies.<sup>31,32</sup> Another model, ADDED dimer-row (ADD), was first suggested in an early study by Hara *et al.*<sup>28</sup> This configuration, with one Si ad-dimer per unit cell [Fig. 2(b)], corresponds to the measured coverage for the  $(3 \times 2)$  and  $(5 \times 2)$  reconstructions. However, though it appears consistent with several experimental data, both empirical<sup>33</sup> and *ab initio*<sup>20</sup> calculations have shown that it is not energetically favored. Furthermore, STM investigations do not support this model.<sup>24,31</sup> Another  $\frac{1}{3}$  coverage model, the ALTERNATE dimer-row (ALT), was proposed by Yan *et al.*<sup>20</sup> This configuration is supported both by calculations<sup>20,33</sup> and by STM studies.<sup>31,32</sup> However, it cannot account for the observed relation between single domain LEED patterns with  $(2 \times 1)$  and  $(3 \times 2)$  periodicities.<sup>3,34</sup> It also fails to explain the  $(3 \times 1)$  reconstruction observed after O or H adsorption.<sup>23,24</sup> Here we have considered only models with Si ad-dimers which are perpendicular to the

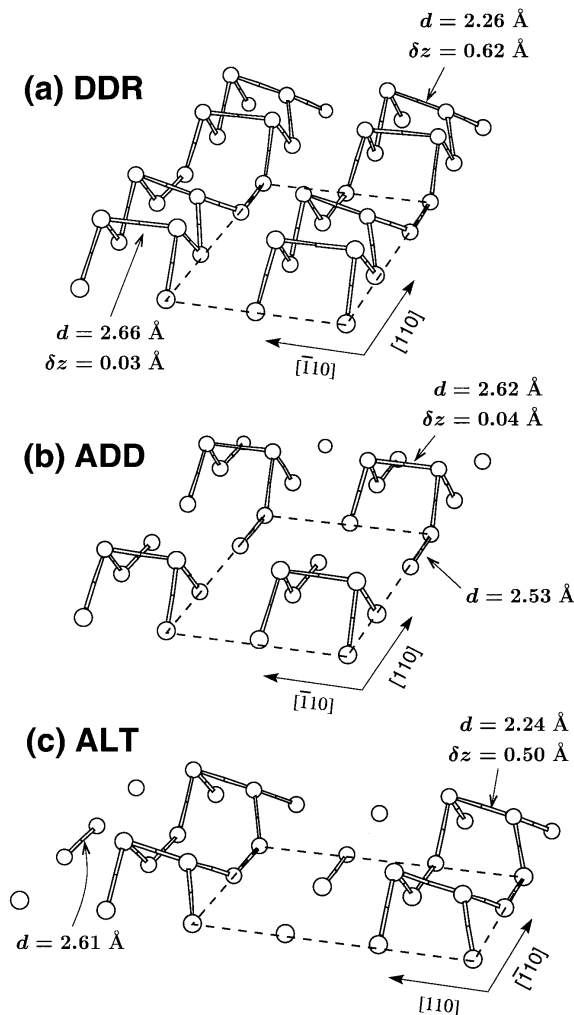


Fig. 2. Ball-and-stick representation of the relaxed atomic structures for the DDR (a), ADD (b) and ALT (c) models of the  $(3 \times 2)$ -reconstructed surface of SiC(001).  $d$  and  $\delta z$  are the distance and height difference between ad-atoms, respectively. Only the ad-layer and the first underlying Si layer are shown for clarity.

dimers on the underlying Si surface. Indeed, our calculations have shown that a single parallel ad-dimer is energetically much less favored than a perpendicular one.

The relaxed atomic structures computed for the three models are shown in Fig. 2. In the DDR geometry, one ad-dimer is strongly tilted ( $\delta z = 0.62$  Å) and has a short bond length ( $d = 2.26$  Å) while the other, weakly bound ( $d = 2.66$  Å), is almost flat ( $\delta z = 0.03$  Å). The inequivalence of the two ad-dimers disagrees with simple expectations<sup>23,24</sup> and with previous calculations by Kitabatake *et al.*, who

found two flat ad-dimers for the DDR model.<sup>35</sup> A single flat and weakly bonded ad-dimer ( $d = 2.62 \text{ \AA}$ ) is obtained in the ADD model, the geometry being close to that previously obtained by Yan *et al.* in a calculation similar to ours.<sup>20</sup> Finally, in the ALT model, the ad-dimer is strongly tilted ( $\delta z = 0.5 \text{ \AA}$ ) and strongly bound ( $d = 2.24 \text{ \AA}$ ), in good agreement with previous calculations.<sup>20</sup> The length of the weak Si dimers in the underlying surface layer is close to the value computed for the  $(2 \times 1)$  reconstruction.

Total energies of the three models of Fig. 2 have been compared using the grand canonical scheme.<sup>36</sup> We found that the ALT model is the most stable configuration over the entire allowed range of the Si chemical potential. However, the energy difference between ALT and DDR obtained under Si-rich conditions is only 77 meV per  $(3 \times 2)$  cell, i.e. within our

error bar (estimated to be 0.3 eV from cutoff and Brillouin zone sampling tests). These results are in agreement with recent localized orbital total energy calculations.<sup>37</sup>

Several experimental STM studies of the  $(3 \times 2)$  reconstruction are currently available.<sup>24,31,38,39</sup> In order to make contact with these experiments, filled states constant-current STM images of the three models of Fig. 2 have been calculated. Representative images are shown in Fig. 3. In both the DDR and ADD models we find strings of peanut-shaped spots, originating from a slight overlap between maxima on adjacent flat ad-dimers. For the DDR model, additional maxima are located on the up adatoms of the tilted ad-dimers. The resulting images are incompatible with the experimental observations of a single oval spot per  $3 \times 2$  cell, stretched in the  $[110]$  direction. On the other hand, in the ALT model the spread-out stretched spots located above up adatoms of the tilted ad-dimers are in accord with experimental STM images of filled states.<sup>31</sup> In view of our energy and STM calculations, the ALT model is likely to be the structure underlying the  $(3 \times 2)$  reconstruction.

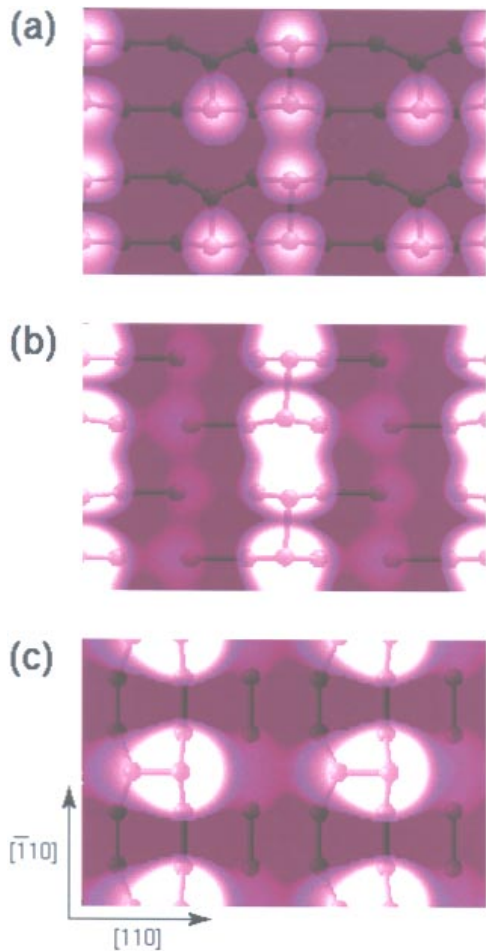


Fig. 3. Calculated constant-current STM images (bias  $V = -1 \text{ V}$ ) for the DDR (a), ADD (b) and ALT (c) models of the  $(3 \times 2)$ -reconstructed surface of SiC(001).

### 3. N Adsorption

With the aim of modeling the initial stages of cubic nitrides growth on  $\beta$ -SiC, we have investigated<sup>8</sup> the deposition of nitrogen atoms on the Si-terminated (001) surface [Si-SiC(001)], by means of first-principles simulations.<sup>40</sup>

In our simulations, we first placed N atoms on top of the Si-SiC(001) surface in selected sites, at a fixed distance ( $2.2 \text{ \AA}$ ) from the Si atoms of the substrate; the potential energy of the whole slab was then optimized so as to determine the configuration of minimum energy. No attempt was made to evaluate energy barriers. We considered coverages of  $1/8$ ,  $1/2$  and 1 monolayer (ML). In all cases, the initial condition for the substrate was the dimer row  $p(2 \times 1)$  reconstruction of Si-SiC(001).<sup>11,13,15</sup> The structural properties of this surface can be easily changed upon application of stress,<sup>11</sup> creation of defects,<sup>6,15</sup> and variation of the temperature.<sup>41</sup> It is therefore likely that important rearrangements of the substrate can occur upon N deposition.

In Fig. 4 we show a top view of the  $p(2 \times 1)$  reconstruction of SiC(001) within our  $c(4 \times 4)$  2D cell.

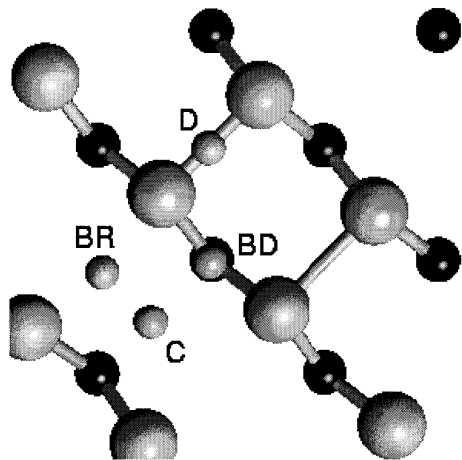


Fig. 4. Nitrogen adsorption sites on the  $p(2 \times 1)$  reconstructed Si-SiC(001) surface (see text). Si and C atoms are represented as gray and black spheres, respectively. N is represented as a small gray sphere. Site D is on top of a surface dimer. Sites BD (Between Dimers) and BR (Between Rows) are between two dimers within or in adjacent dimer rows, respectively. On an ideal surface sites D and BR are equivalent. Site C is a hollow site at equal distance from four surface Si atoms. Adsorption at sites D and BR corresponds to the continuation of the zinc blende stacking sequence of (001) planes (ABCA); we call these sites zinc blende sites.

The projections on a (001) plane of the N adsorption sites are indicated. For a  $1/8$  ML coverage, we found that the zinc blende sites (D and BR) are degenerate in energy and correspond to the most stable configuration. On an ideal surface D and BR sites would be exactly equivalent and it is not surprising that they are degenerate in energy for a surface like Si-SiC(001), exhibiting a very weak reconstruction. The C configuration (see Fig. 4) is unstable (an adatom placed in C spontaneously moves to the site BR), whereas BD is a metastable geometry about  $1$  eV/adatom higher in energy than that of the zinc blende sites. In the equilibrium geometry (D or BR), the relaxation mechanism observed at the surface involves mostly the adsorbate and two neighboring Si atoms, which we will call a *nitridized Si pair*. In the optimized configuration, N-Si distances are  $1.7$  Å, slightly shorter than the corresponding bond length in  $\text{Si}_3\text{N}_4$  ( $1.74$  Å).<sup>42</sup> In both BR and D sites, the distance between Si atoms immediately below the adatom is slightly smaller than on the clean surface; on the other the dimers adjacent to N atoms are significantly elongated, with Si atoms essentially occupying

the positions of an ideal surface. At  $1/8$  ML coverage, the highest occupied electronic states are antibonding states originating from Si dimers, similar to the clean  $p(2 \times 1)$  reconstruction.<sup>11</sup>

At a coverage of  $1/8$  ML we have also carried out a calculation with 16 atoms/layer and two nitrogen adsorbates. We observed the formation of two areas with identical structure around each N atom, having the same geometry as the one determined with our 1 ad-atom/layer calculation.

At a coverage of  $1/2$  nitrogen ML, we have studied adsorption at the sites BD and BR, i.e. corresponding to the metastable and stable sites for  $1/8$  ML coverage. Upon adsorption of all nitrogen atoms at BR sites, we observed the formation of nitridized Si pairs; adsorbing all nitrogen atoms at BD sites yields instead a metastable configuration which is about  $1$  eV/adatom higher in energy than that of BR sites. These results are similar to those obtained for a  $1/8$  ML coverage. However, structural changes in the substrate are more significant at  $1/2$  than at  $1/8$  ML. The N-Si distances are  $1.62$ – $1.69$  Å (smaller than in the case of  $1/8$  monolayer) and the Si pairs under the adatoms are buckled, i.e. Si atoms change their relative coordinate in the direction perpendicular to the surface by about  $0.1$  Å. We can picture the surface as fully covered with a periodic arrangement of nitridized buckled Si pairs. At this coverage the electronic states close to the top of the valence band are localized on the N ad-atoms.

We also studied a configuration in which N forms  $\text{N}_2$  dimers, with each nitrogen being threefold-coordinated and bonded to two Si atoms. This configuration is only  $0.06$  eV/adatom higher in energy than that of nitridized Si pairs.

The energetics of N adsorbed on Si-SiC(001) changes dramatically when going to a coverage of 1 ML. We have considered adsorption at all the sites displayed in Fig 4. Nitrogen atoms can be adsorbed at zinc blende sites, but these correspond to a metastable configuration. When heating the system to about  $500$  K, the ad-atoms rearrange so as to form long ( $1.59$  Å) unbuckled  $\text{N}_2$  dimers, with each N bonded to two Si atoms, in a hydrazine-like arrangement ( $\text{N}_2\text{H}_4$  is a nonplanar molecule, with N-N distance equal to  $1.47$  Å). We call this configuration a nitrogen wet surface. This geometry, shown in Fig. 5, is  $0.75$  eV/atom lower in energy than the metastable zinc blende geometry. The N-Si bonds ( $1.82$  Å) are

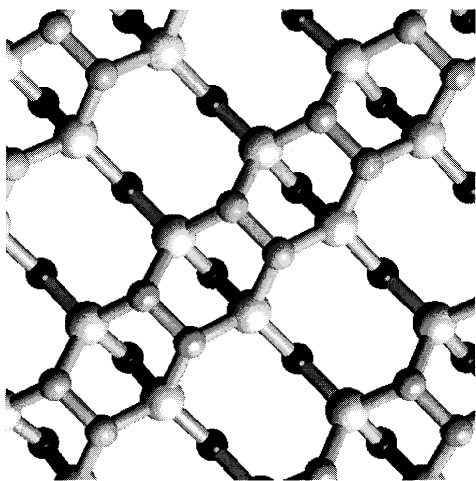


Fig. 5. Top view of the Si-SiC(001) surface covered by one nitrogen monolayer. Si and C atoms are represented as gray and black spheres, respectively. N is represented as a small gray sphere. The arrangement of  $N_2$  dimers in a  $p(2 \times 1)$  pattern on top of the surface is apparent.

longer than in nitridized Si pairs and the Si-N-Si bond angles are slightly larger ( $\approx 112^\circ$ , against  $108^\circ$ ). While the bond length of Si-Si surface dimers is not substantially modified (2.6 Å), some Si-C bonds are considerably elongated (up to 1.90 Å), thus modifying the ionicity of heteropolar bonds close to the surface. In this stable configuration the first surface layer is perfectly coated, with no dangling bonds, yielding an inert, insulating substrate. The computed energy gap between valence and conduction states is about 1 eV. Given the usual underestimate of energy gaps obtained within the LDA approximation, we expect the actual gap to be larger than 1 eV. The states at the top of the valence band (see Fig. 6) are spatially localized on N atoms and exhibit a lone pair character, similar to that of the highest occupied state of the  $N_2H_4$  molecule. These are shown in Fig. 7.

We also considered other geometrical arrangements of 1 ML adatoms, to investigate whether interface mixing could be energetically favored. When N adatoms are placed on top of Si atoms, they relax towards a disordered structure, much higher in energy than that of the metastable zinc blende geometry. Indeed, in this disordered geometry a large number of dangling bonds are not saturated. On the other hand, placing N in C sites (see Fig. 4) leads to interface mixing: N is incorporated into the substrate and

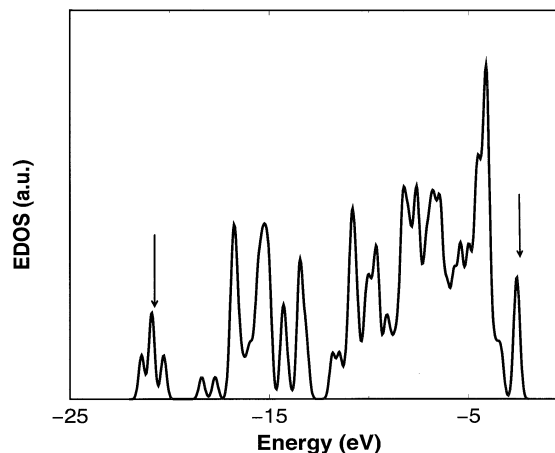


Fig. 6. Electronic density of occupied states of the SiC slab terminated by one nitrogen monolayer. Nitrogen 2s states are located at the bottom of the valence band (see arrow on the left hand side), whereas nitrogen lone-pair-like states (see Fig. 4) are at the top of the valence band (see arrow on the right hand side), giving rise to a distinctive peak which is absent in the clean, uncoated surface.

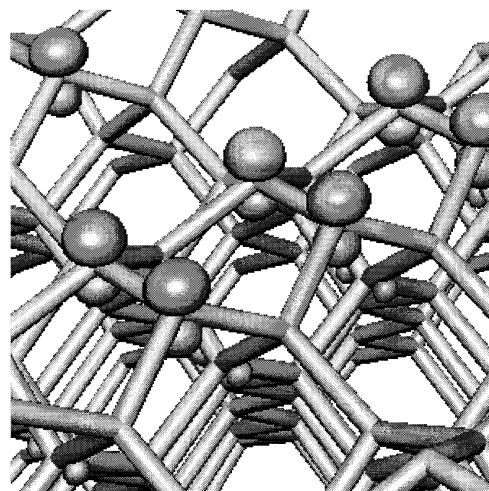


Fig. 7. Plot of the square modulus of the highest occupied orbital of the slab, localized on N atoms. Only bonds between atoms are displayed.

both N-C and N-Si bonds are formed. The mixed interface with lowest energy was found when heating the whole slab at 300 K, during the optimization procedure. This configuration is about 0.2 eV higher in energy than the metastable zinc blende geometry.

In order to investigate whether a full nitridization of the Si-SiC(001) surface is favored from an energetic point of view, we computed the binding energy

Table 1. Binding energies ( $E_b$ ) of the nitridized Si-SiC(001) surface as a function of coverage, referred to the value obtained for 1/8 ML.  $E_b = [E_{N-SiC} - E_{SiC}]/n - E_{N_2}/2$ , where  $E_{N-SiC}$  and  $E_{SiC}$  are respectively the total energies of the nitridated and of the clean, reconstructed Si-terminated SiC(001).  $E_{N_2}$  is the computed total energy of the  $N_2$  molecule and  $n = 2, 8, 16$  is the number of N atoms in our slab (containing two equivalent surfaces) at 1/8, 1/2 and 1 ML coverage, respectively. The binding energy obtained at 1/8 ML is  $-1.2$  eV; this number is expected to be an overestimate of the binding energy since the LDA error on the binding of the  $N_2$  molecule is expected to be larger than that on the binding of N to the surface.

Coverage	Geometry	$E_b$ (eV/ad-atom)
1/8	nitridized Si pairs	0.0
1/2	nitridized Si pairs	-0.1
1	nitridized Si pairs	+0.35
1	nitrogen wet surface	-0.4

of the surface, against dissociation into the  $p(2 \times 1)$ -reconstructed substrate and  $N_2$  molecules, as a function of coverage. Our results are displayed in Table 1. We find that a 1 ML coverage is unfavored if N atoms sit in zinc blende adsorption sites, while it is favored for a nitrogen wet surface. Experimentally,<sup>43,44</sup> full nitridization of the Si-SiC(001) surface was not observed for coverages higher than 0.6–0.7 ML, when operating at high temperature ( $T \simeq 800$ – $1000^\circ\text{C}$ ). This may indicate that under these conditions zinc blende sites become stable and that nitrogen wetting of the surface can be achieved only at low temperature.

#### 4. Conclusion

To summarize, we have performed plane-wave pseudopotential calculations for the deposition of Si and N atoms on the Si-terminated SiC(001) surface.

Regarding Si adsorption, we found that a Si ad-dimer perpendicular to the underlying  $p(2 \times 1)$  row is favored compared to a parallel one. We have investigated three different structural models for the  $(3 \times 2)$ -reconstructed  $\beta$ -SiC(001) surface. Our energy and STM calculations favor the ALT model and exclude the DDR and ADD models, although some ambiguities remain.

In the second part of the paper, we have investigated the nitrogen deposition on SiC(001). For

coverages less than and equal to a 1/2 monolayer, nitrogen atoms are preferably adsorbed at zinc blende sites and form nitridized Si pairs. At 1/2 ML the formation of these complexes significantly modifies the  $p(2 \times 1)$  reconstruction of the substrate, leading to changes in the bonding of surface dimers. At 1 ML, zinc blende absorption sites are metastable: our finite temperature simulations predict the formation of hydrazine-like  $N_2Si_4$  complexes coating the first surface layer. Only in this configuration is full nitridization of the surface energetically favored. Our results indicate that prenitridization of SiC substrates is an undesirable feature in nitride growth, leading to a complete surface coating. Finally, we note that wetting SiC surfaces with nitrogen could be used to enhance the mechanical properties of crystalline SiC,<sup>45</sup> similar to amorphous SiC.<sup>46</sup>

#### Acknowledgments

We are grateful to A. Rizzi, V. M. Bermudez, P. Soukiassian and G. Dujardin for fruitful discussions. L. P. acknowledges the Swiss National Foundation program NFP36 and the Italian National Research Council (CNR) for financial support. Work done at the Lawrence Livermore National Laboratory under the auspices of the U.S. Department of Energy, Office of Basic Energy Sciences, Division of Materials Science, Contract No. W-7405-ENG-48, and at the Swiss Center for Scientific Computing (CSCS).

#### References

1. H. Morkoç, S. Strite, G. B. Gao, M. E. Lin, B. Sverdlov and M. Burns, *J. Appl. Phys.* **76**, 1363 (1994).
2. Proceedings of the 1995 MRS Fall Meeting, *Gallium Nitride and Related Materials*, eds. F. A. Ponce *et al.* (Material Research Society, 1995).
3. V. M. Bermudez, *Phys. Stat. Sol. (b)* **202**, 447 (1997).
4. G. Feuillet, H. Hamaguchi, K. Ohta, P. Hacke, H. Okumura and S. Yoshida, *Appl. Phys. Lett.* **70**, 1025 (1997).
5. R. B. Capaz, H. Lim and J. D. Joannopoulos, *Phys. Rev.* **B51**, 17755 (1995); L. K. Teles, L. M. R. Scolfaro, R. Enderlein, J. R. Leite, A. Josiek, D. Schikora and K. Lischka, *J. Appl. Phys.* **80**, 6322 (1996); R. Di Felice, J. E. Northrup and J. Neugebauer, *Phys. Rev.* **B54**, R17351 (1996); R. Di Felice and J. E. Northrup, *Phys. Rev.*

- B56**, 9213 (1997); P. Ferrara, N. Binggeli and A. Baldereschi, *Phys. Rev.* **B55**, R7418 (1997).
6. A. Catellani, G. Galli and F. Gygi, *Appl. Phys. Lett.* **72**, 1902 (1998).
  7. L. Pizzagalli, A. Catellani, G. Galli, F. Gygi and A. Baratoff, to be published in *Phys. Rev. B* (1999).
  8. G. Galli, A. Catellani and F. Gygi, to be published in *Phys. Rev. Lett.* (1999).
  9. D. R. Hamann, *Phys. Rev.* **B40**, 2980 (1989).
  10. J. Tersoff and D. Hamann, *Phys. Rev.* **B31**, 805 (1985).
  11. A. Catellani, G. Galli, F. Gygi and F. Pellacini, *Phys. Rev.* **B57**, 12255 (1998).
  12. M. Sabisch, P. Krüger, A. Mazur, M. Rohling and J. Pollmann, *Phys. Rev.* **B53**, 13121 (1996).
  13. J. Powers, A. Wander, M. A. Van Hove and G. A. Somorjai, *Surf. Sci. Lett.* **260**, L7 (1992).
  14. P. Käckell, F. Bechstedt, H. Hüskén, B. Schröter and W. Richter, *Surf. Sci.* **391**, L1183 (1997).
  15. P. Soukiassian, F. Semond, G. Dujardin, A. Mayne, L. Douillard, L. Pizzagalli and C. Joachim, *Phys. Rev. Lett.* **78**, 907 (1997).
  16. J. Kitamura, S. Hara, H. Okushi, S. Yoshida, S. Misawa and K. Kajimura, *Proc. of the 15th Symposium on "Materials Science and Engineering Research Center of Ion Beam Technology"* (Hosei Univ., 1997).
  17. L. Pizzagalli, C. Joachim, A. Mayne, G. Dujardin, F. Semond, L. Douillard and P. Soukiassian, *Thin Solid Films* **318**, 136 (1998).
  18. G. Brocks, P. J. Kelly and R. Car, *Phys. Rev. Lett.* **66**, 1729 (1991).
  19. F. Semond, P. Soukiassian, A. Mayne, G. Dujardin, L. Douillard and C. Jaussaud, *Phys. Rev. Lett.* **77**, 2013 (1996).
  20. H. Yan, A. Smith and H. Jónsson, *Surf. Sci.* **330**, 265 (1995).
  21. P. Soukiassian, F. Semond, A. Mayne and G. Dujardin, *Phys. Rev. Lett.* **79**, 2498 (1997).
  22. The optimized geometry of the ad-dimer parallel to the  $(2 \times 1)$  rows gives a buckled dimer of length 2.24 Å, with atoms sitting 1.9 and 1.35 Å from the surface, consistently with the results reported in Ref. 21.
  23. M. Dayan, *J. Vac. Sci. Technol.* **A4**, 38 (1985).
  24. S. Hara, S. Misawa, S. Yoshida and Y. Aoyagi, *Phys. Rev.* **B50**, 4548 (1994).
  25. J. Kitamura *et al.* (unpublished).
  26. H. W. Yeom, Y.-C. Chao, S. Terada and R. I. G. Uhrberg, *Phys. Rev.* **B56**, R15525 (1997).
  27. H. W. Yeom, Y.-C. Chao, I. Matsuda, S. Hara, S. Yoshida and R. I. G. Uhrberg, *Phys. Rev.* **B58**, 10540 (1998).
  28. S. Hara, W. F. J. Slijkerman, J. F. van der Veen, I. Ohdomari, S. Misawa, E. Sakuma and S. Yoshida, *Surf. Sci. Lett.* **231**, L196 (1990).
  29. T. Yoshinobu, I. Izumikawa, H. Mitsui, T. Fuyuki and H. Matsunami, *Appl. Phys. Lett.* **59**, 2844 (1991).
  30. S. Hara, Y. Aoyagi, M. Kawai, S. Misawa, E. Sakuma and S. Yoshida, *Surf. Sci.* **273**, 437 (1992).
  31. F. Semond, P. Soukiassian, A. Mayne, G. Dujardin, L. Douillard and C. Jaussaud, *Phys. Rev. Lett.* **77**, 2013 (1996).
  32. P. Soukiassian, F. Semond, A. Mayne and G. Dujardin, *Phys. Rev. Lett.* **79**, 2498 (1997).
  33. H. Yan, X. Hu and H. Jónsson, *Surf. Sci.* **316**, 181 (1994).
  34. R. Kaplan, *Surf. Sci.* **215**, 111 (1989).
  35. M. Kitabatake and J. E. Greene, *Appl. Phys. Lett.* **69**, 2048 (1996).
  36. G.-X. Qian, R. M. Martin and D. J. Chadi, *Phys. Rev.* **B38**, 7649 (1988).
  37. R. Gutierrez, M. Haugk, J. Elsner, G. Jungnickel, M. Elstner, A. Sieck, Th. Frauenheim and D. Porezag, *Phys. Rev.* **B60**, 1771 (1999).
  38. S. Hara, J. Kitamura, H. Okushi, S. Misawa, S. Yoshida and Y. Tokumaru, *Surf. Sci.* **357–358**, 436 (1996).
  39. S. Hara, J. Kitamura, H. Okushi, S. Misawa, S. Yoshida, K. Kajimura, H. W. Yeom and R. I. G. Uhrbert, *Surf. Sci.* **421**, L143 (1999).
  40. R. Car and M. Parrinello, *Phys. Rev. Lett.* **55**, 2471 (1985).
  41. V. Yu. Aristov, L. Douillard, O. Fauchoux and P. Soukiassian, *Phys. Rev. Lett.* **79**, 3700 (1997).
  42. R. W. G. Wyckoff, *Crystal Structures* (Interscience, New York, 1964).
  43. V. Bermudez, *Surf. Sci.* **276**, 59 (1992).
  44. V. van Elsbergen, M. Rohleder and W. Moñich, *Appl. Surf. Sci.* **134**, 197 (1998).
  45. N. Rajan, C. A. Zorman, M. Mehregany, R. DeAnna and R. Harvey, *Thin Solid Films* **315**, 170 (1998).
  46. A. L. Yee, H. C. Ong, F. Xiong and R. Chang, *J. Mater. Res.* **11**, 1979 (1996).